Research Article

Manganese- and Iron-Doped Zinc Oxide for Photocatalytic Degradation of Recalcitrant Dyes

Sandhya Babel*, Hanggara Sudrajat and Ajay Aby Abraham
School of Biochemical Engineering and Technology,
Sirindhorn International Institute of Technology, Thammasat University,
Pathum Thani 12120, Thailand

Abstract

Mn- and Fe-doped ZnO are synthesized by modified sol-gel method. The as-synthesized catalysts are characterized by Fourier transform infrared (FTIR) spectroscopy, scanning electron microscopy (SEM) and energy dispersive X-ray (EDX) spectroscopy. Their photocatalytic activity is investigated for the degradation of methylene blue (MB) and amaranth (AM) under UVA and visible light. The results show that the doping of Mn and Fe generally leads to enhanced photocatalytic activity. However, compared to Fe-doped ZnO, pristine ZnO prepared from zinc acetate (acet-ZnO) shows better performances. For instance, using 1 g/L of catalyst under UVA light, the MB degradation with acet-ZnO and Fe-ZnO are 98 and 43% in 90 min at pH 7, respectively. Adsorption of dye insignificantly contributes to the dye removal. Less than 5% of dyes are adsorbed within 2 h in the absence of light. Furthermore, Mn doping is more effective in enhancing the photocatalytic activity. UVA is found to be a better light source for all the catalysts. Using UVA light, 5 mol% Fe-ZnO with concentration of 1 g/L can degrade 93% of AM in 90 min at pH 7. Using visible light under identical experimental conditions, 10 mol% Mn-ZnO gives 50% efficiency for the AM degradation. In all the cases using doped ZnO, the dye degradation increases with increasing catalyst concentration and irradiation time and decreases with increasing dye concentration. Increasing pH generally increases the dye degradation up to an optimum value. Moreover, the MB and AM degradation by Fe-ZnO under visible light mainly occurs through a self-sensitization mechanism instead of oxidation by reactive species. Overall, the developed catalysts are able to efficiently degrade MB and AM in a short period of time. However, they are not that reusable. Therefore, proper techniques are required for regeneration so as to achieve appreciable reusability.

Keywords: metal doping; sol-gel process; zinc oxide; photocatalyis; dye degradation

1. Introduction

Dyes are widely employed in the textile industry. During the dyeing process, dyes can be released into the water bodies due to low process efficiency and improper treatment of effluents [1]. These lead to serious environmental problems and aesthetic issues. Because of their effectiveness for dye removal, coagulation, filtration, and adsorption with activated carbon are extensively used [2]. However, they merely involve transfer of the dyes from one phase to another. Biological treatment is a cost-effective method. But, the majority of

***Correspondence :** sandhya@siit.tu.ac.th
DOI 10.14456/tijsat.2016.28

dyes are resistant to biological process [3]. Thus, finding an effective, yet sustainable method for dye wastewater treatment is an important concern.

Semiconductor photocatalysis is a promising method since it offers a clean, solar-driven process for dye wastewater treatment [4]. Based on literature, it is possible to apply photocatalytic process in real wastewater [5, 6]. The photocatalytic process is normally integrated with other processes to reduce turbidity of wastewater. Some pilot plants involving the photocatalytic process are now in operation. Among semiconductor materials, metal oxides are the best choice due to their distinctive properties, high stability, and cost effectiveness [7]. For degradation of organic compounds, the valence band (VB) potential of metal oxide should be as low as possible to allow the generation of holes with strong oxidation power [8]. Holes with strong oxidation power can effectively degrade the surface-adsorbed organic pollutant and are also able to make the oxidation of surface hydroxyl group or water into hydroxyl radical thermo-dynamically favourable. Therefore, the VB features of a metal oxide play a critical role.

Among semiconductors, ZnO has emerged to be a more efficient catalyst for environmental remediation since it is able to produce reactive species more efficiently for oxidation of organic compounds [9]. Also, it has greater numbers of active sites with high surface reactivity [10]. ZnO has been shown to be an improved catalyst as compared to commercialized TiO_2 based on the larger initial activity rates [11] and its absorption efficacy under solar irradiation [12]. But, ZnO has almost the same band gap (3.2 eV) as TiO_2 and hence can only absorb UV light. This consequently limits its practical applications in a real setting under solar light.

For enhancement of photocatalytic activity of pristine ZnO, especially under visible light, metal doping can be an effective method. Doping with Mn [13] and Fe [14] were reported to be beneficial for the enhancement of photocatalytic activity of ZnO. Nevertheless, the enhancement of photocatalytic activity is not always achieved since it greatly depends on the preparation method employed. A wide range of methods, such as sputtering deposition technique [15], chemical vapour deposition [16], and various hydrothermal procedures [17] have been used. Unfortunately, such methods need sophisticated equipment, strictly controlled conditions, high temperatures and even high vacuums. Hence, discovering a low cost method for metal-doped ZnO is of great importance. One of the promising methods which is inexpensive and facile and does not involve harsh experimental conditions is the sol-gel method.

This research aims to improve dye degradation efficiency by doping with Mn and Fe through novel routes based on the precipitation of precursors in aqueous media. The Mn and Fe doping are expected to improve the photocatalytic activity both under visible and UV light. The as-synthesized catalysts were evaluated for the degradation of two recalcitrant dyes, namely methylene blue (MB) and amaranth (AM), under UVA and visible light. These dyes are widely employed by the textile industry [18, 19] and thus very likely to be present in textile wastewater. The effects of operating parameters on the dye degradation efficiency as well as the reusability of the catalysts were also investigated.

2. Materials and Methods

2.1 Chemicals

All chemicals were of analytical grade. Iron (III) nitrate (Ajax), zinc acetate (Aldrich), manganese (II) sulphate (Ajax), oxalic acid (Aldrich), methylene blue (Merck), and amaranth (Aldrich) were used as received without further purification. DI water was used in all the process.

2.2 Synthesis of Fe-ZnO

First, 5.487 g of zinc acetate was added into 100 mL of DI water to form solution A, which then was heated in the water bath at 65 ºC for 30 min. Meanwhile, solution B was formed by adding 6.3035 g of oxalic acid to 50 mL of DI water. A required amount of iron (III) nitrate was dissolved in 20 mL of DI water for doping of 1%, 5% and 10% mol of Fe, respectively. Subsequently, solution B was added into solution A until the gel was formed. The gel was calcined at 500 ºC for 2 h. The obtained powder of Fe-ZnO was then kept in a desiccator for further use. Pristine ZnO was also synthesised using the same process, but without addition of iron (III) nitrate, denoted as acet-ZnO.

2.3 Synthesis of Mn-ZnO

First, 8.477 g of zinc nitrate was mixed with 20 mL of DI water. A required amount of manganese (II) sulphate was added into the zinc nitrate solution to get 1%, 5% and 10% mol of Mn doping. Subsequently, 30 mL of 2 M NaOH was added to the solution until the gel was formed. The obtained powder of Mn-ZnO was then kept in a desiccator for further use. Pristine ZnO was also synthesised using the same process, but without the addition of manganese (II) sulphate, denoted as nit-ZnO.

2.4 Characterization

The infrared spectra were recorded by a Fourier transform infrared (FTIR) spectrometer (Thermo Nicolet, iS5). The morphological properties were observed by scanning electron microscopy (SEM) (Hitachi, S-3400N) coupled with energy dispersive X-ray (EDX) for elemental analysis.

2.5 Photocatalytic activity evaluation

The photocatalytic activity of the catalyst was evaluated for the degradation of AM and MB under visible and UVA light in a batch slurry system. A suspension (0.1 L) containing known concentrations of the dye and the catalyst was transferred into a batch photoreactor and magnetically stirred in the dark to attain equilibrium. A 12 W fluorescent lamp and a 10 W blacklight lamp were used as visible and UVA light sources, respectively. The average visible light irradiance and UV light irradiance at the topmost surface of the suspension were 40 W/m^2 and 4.7 W/m^2, respectively. The lamp was switched on to initiate a photocatalytic reaction. After a given irradiation time, the suspension was withdrawn and centrifuged to measure the absorbance of MB solution at λ_{max} of 664 nm or AM solution at λ_{max} of 521 nm by using a spectrophotometer. To determine the dye concentration, calibration plots based on the Beer-Lambert's law were established by relating the absorbance to the concentration. The dye degradation efficiency was calculated from the equation:

$$Degradation\ (\%) = [(C_0 - C)/C_0] \times 100 \qquad (1)$$

Where, C_0 and C are the initial dye concentration and dye concentration after irradiation (mg/L), respectively. The adsorption ability of the catalyst was also evaluated. Adsorption of MB and AM on the catalyst was conducted in the absence of light at room temperature. It was found that less than 5% of dyes are adsorbed within 2 h under dark conditions indicating low adsorption ability of the catalyst. To study the effect of operating parameters on the dye degradation, the experiments were performed by varying key operating parameters, namely catalyst concentration, irradiation time and pH. The catalyst reusability was evaluated by recycling the catalyst twice under the same experimental conditions. All of the experiments were replicated twice under identical conditions and the results were presented as a mean of two experiments.

3. Results and Discussion

3.1 Surface functional groups and morphological properties

Figure 1 shows the FTIR spectra of pristine and doped ZnO samples. There are broad peaks at 3450 cm^{-1}, corresponding to the surface-adsorbed water. The peak intensities at around 1630 cm^{-1}

corresponding to hydroxyl groups are not that strong [20]. This indicates low population of hydroxyl groups on the surface. Moreover, the peaks at around 500 cm^{-1} were assigned to the Zn-O bond. The peak that was obtained for Fe-ZnO at around 1100 cm^{-1} could be attributed to the incorporation of Fe ions into the lattice structure of ZnO. A similar peak was also observed in the FTIR spectrum of Mn-ZnO at around 1100 cm^{-1}. However, the peak intensity is not that strong due to the presence of an additional, very strong peak belonging to Na impurities at around 1380 cm^{-1}. The presence of Na impurities may be detrimental to photocatalytic activity. Thus, it is recommended to replace NaOH as the precipitating agent with aqueous ammonia.

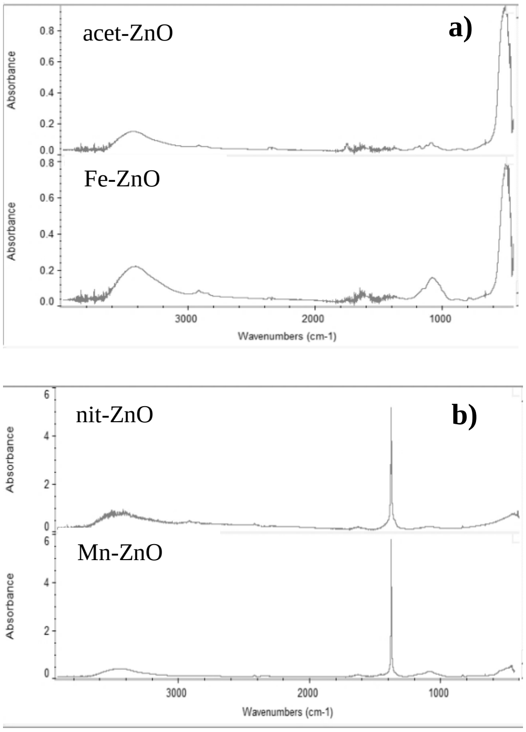

Figure 1. FTIR spectra of the catalysts.

Figure 2 shows the SEM images of pristine and doped ZnO samples. The images show that the catalysts are irregular in shape with rough surfaces. There is no significant alteration on the particle morphology after Fe doping. Whereas, after doping with Mn, the size of the particles seems to decrease quite significantly. The decreased particle size is actually beneficial for photocatalytic activity. This is because rapid migration of photoproduced electrons and holes to the catalyst surface is guaranteed, leading to low probability of bulk recombination. Also, decreased particle size is typically accompanied by increased specific surface area of catalyst particles, which is obviously useful for adsorption of reactant and absorption of the incoming light.

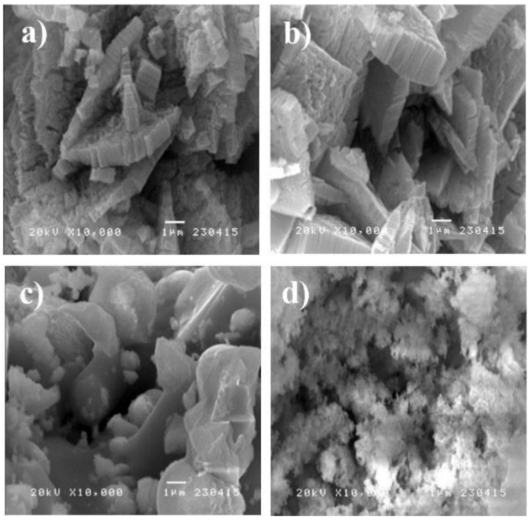

Figure 2. SEM images of acet-ZnO (a), 5 mol% Fe-ZnO (b), nit-ZnO (b) and 5 mol% Mn-ZnO (d).

Table 1 and Table 2 show elemental compositions of pristine and doped ZnO. The presence of Fe and Mn are confirmed by EDX. The presence of Na impurities is also observed. This is in agreement with the FTIR results. The Na impurities exist in the ZnO structure, likely due to inappropriate washing of particles after synthesis.

Table 1. Elemental composition of pristine and 5 mol% Fe-ZnO.

	acet-ZnO		5 mol% Fe-ZnO	
Element	Weight (%)	Atomic (%)	Weight (%)	Atomic (%)
Zn	80.34	50	82.88	57.57
O	19.66	50	14.07	39.94
Fe			3.05	2.48

Table 2. Elemental composition of pristine and 5 mol% Mn-ZnO.

	nit-ZnO		5 mol% Mn-ZnO	
Element	Weight (%)	Atomic (%)	Weight (%)	Atomic (%)
Zn	75.79	44.72	77.23	47.79
O	20.01	48.24	19.77	50
Na	4.2	7.04		
Mn			3	2.21

3.2 Comparative degradation of dyes

Figure 3 shows the dye degradation efficiencies of the catalysts. In all the cases, the dye degradation is favourable under UVA light. The catalysts are able to achieve appreciable dye degradation efficiencies under UVA light, even for pristine ZnO. Under UVA light, 1 g/L of pristine ZnO can degrade 98% of MB with concentration of 10 mg/L in only 90 min at pH 7. This is understandable since, based on the literature, the maximum light absorption in ZnO is always in the UV region, even after doping with either metal or non-metal [21]. Therefore, more light is absorbed by the catalyst in the UVA region instead of in the visible region for generating reactive species. In addition, charge carriers generated under UVA light possess stronger oxidation power compared to those generated under visible light.

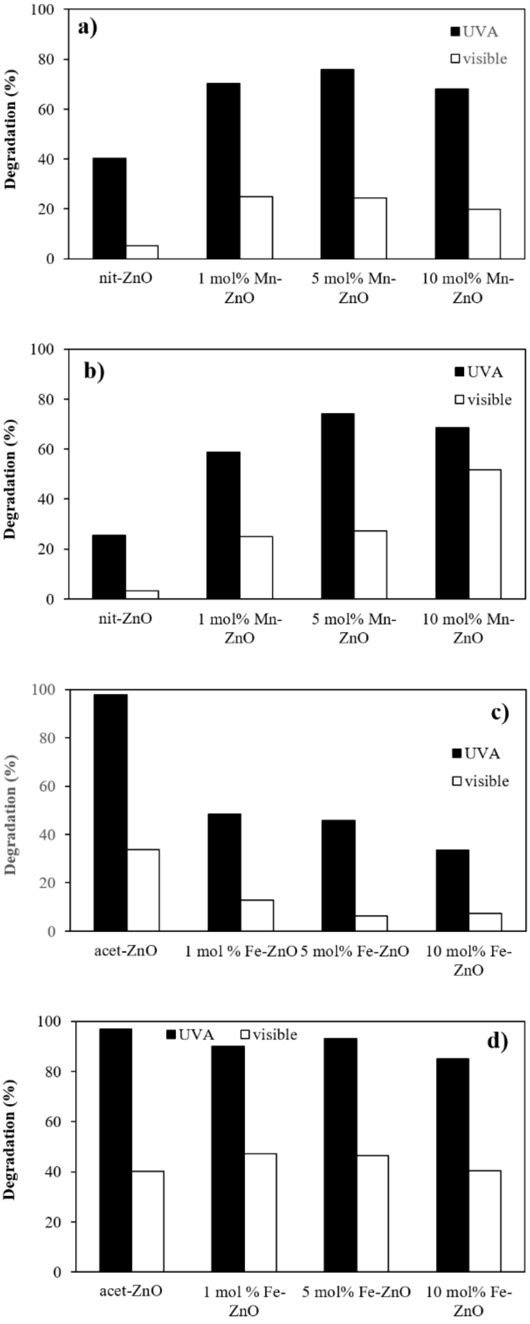

Figure 3. Degradation MB (a, c) and AM (b, d) by pristine and doped ZnO under visible and UVA light (catalyst concentration = 1 g/L, dye concentration = 10 mg/L, pH = 7, and irradiation time 90 min).

As can be seen, both Mn doping and Fe doping are generally beneficial to the dye degradation, except for MB degradation by Fe-ZnO. With increasing dopant content, the dye degradation generally increases up to an optimum value and then decreases. The optimum dopant contents are mostly at 5 mol%. The increase in photo-catalytic activity with increase in dopant content until it reaches the optimum can be explained on the basis of three factors. First, a space charge layer is typically formed on the doped metal oxide surface [22]. This layer is able to separate the photoproduced electrons and holes. With increased dopant content, the surface barrier becomes higher and the electrons and holes within the region are efficiently separated by the large electric field. Second, because of the difference in electron negativity between Zn and metal (Mn or Fe), the Zn–O–metal bonds formed via Mn^{2+} or Fe^{3+} entering into the shallow surface of ZnO enables the electrons and holes to migrate to the ZnO surface [23]. Third, metal ion doping usually results in a lattice deformation and leads to crystal defects [24]. The defects may inhibit the electron-hole recombination. When in excess, the presence of dopant on the surface and in the pores of ZnO may decrease the specific area, block the pores, impede the dye adsorption and ultimately inhibit the dye degradation [25]. In addition, an excess amount of dopant on the surface could screen the ZnO from the light and impede the interfacial transfer of the electrons and holes, leading to fast recombination [26].

Furthermore, in the case of MB degradation, pristine ZnO has much better performance than Fe-ZnO. This is probably because Fe doping increases the positive charge of the ZnO surface. As MB is cationic species in the solution, the increased positive charge of the surface increases the repulsive forces between the catalyst and MB. Thus, MB cannot be effectively adsorbed by the catalyst. All of these factors lead to decreased degradation of MB. It is also interesting to note that pristine ZnO, especially that which is prepared from zinc acetate, is able to degrade AM and MB under visible light, although pristine ZnO is theoretically not visible light active due to its large band gap. This indicates that the dye degradation under visible light by Fe-ZnO mainly occurs through a self-sensitization mechanism instead of oxidation by reactive species. In the self-sensitization mechanism, the excited dye adsorbed on the ZnO surface injects its electron to the conduction band of ZnO after absorbing visible light (Figure 4) [5]. After electron injection, the excited dye becomes a radical anion and subsequently undergoes further oxidation with O_2. On the other hand, the ZnO prepared from zinc nitrate shows negligible dye degradation under visible light. This means that the dye degradation by Mn-ZnO mainly takes place through oxidation by reactive species instead of the self-sensitization mechanism. Such difference in the dye degradation mechanism is most likely due to the difference in the surface properties of the catalyst. Fe-ZnO seems to strongly anchor the dye molecules. Thus, the self-sensitization mechanism is more likely to occur as Fe-ZnO may provide more favourable conditions for the dye adsorption on its surface.

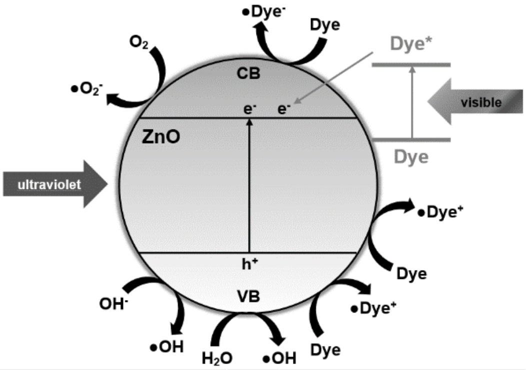

Figure 4. Schematic illustration of charge carrier generation in pristine ZnO upon light irradiation.

3.3 Effect of operating parameter on the dye degradation efficiency

To study the effect of operating parameter on the dye degradation efficiency, some catalysts showing appreciable performances are subjected to further evaluation. The 10 mol% Mn-ZnO and 5 mol% Fe-ZnO were selected for the AM degradation under visible and UVA light, respectively. For the MB degradation under UVA, only 5 mol% Mn-ZnO was selected.

3.3.1 Effect of catalyst concentration

For evaluation of the effect of catalyst concentration on the dye degradation, the catalyst concentration was varied (0.4, 0.6, 0.8 and 1g/L). As shown in Fig. 5, the dye degradation under both visible and UVA light increases as the catalyst concentration increases from 0.4 g/L to 1 g/L. These increases of the dye degradation are due to the fact that with the increase of catalyst concentration, the total surface area for the light absorption and the dye adsorption increases. Therefore, more reactive radicals are generated. For further evaluation, the catalyst concentration is kept constant at 1 g/L since it gives the highest degradation for all the three catalysts.

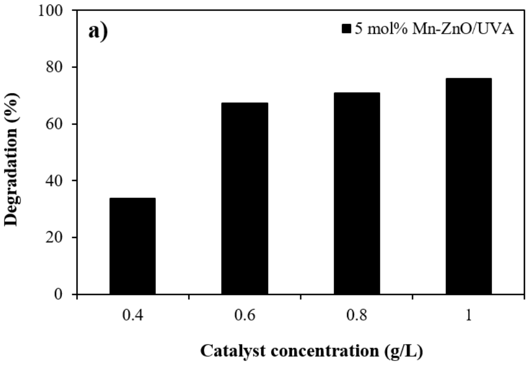

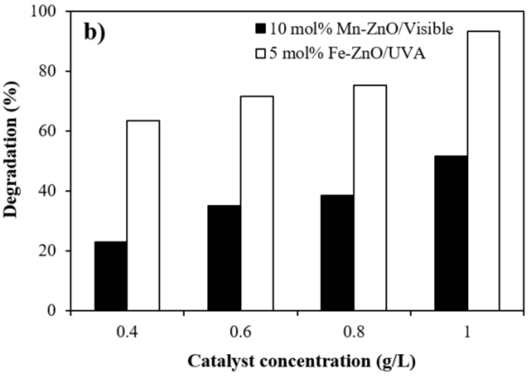

Figure 5. Effect of catalyst concentration on the degradation of MB (a) and AM (b) (pH = 7, dye concentration = 10 mg/L, irradiation time = 90 min).

3.3.2 Effect of irradiation time

Irradiation was evaluated with varied values (30, 60, 90 and 120 min). The percentage of the dye degradation with respect to contact time is shown in Fig. 6. As irradiation time increases, the dye degradation generally increases. This is because more light is absorbed by the catalyst for producing reactive radicals. Thus, more dye molecules are degraded. However, for 10 mol% Mn-ZnO under visible light, there is no increase of the AM degradation when the irradiation time is increased from 90 to 120 min. This may be because the recombination of charge carriers takes place more frequently with increasing contact time [27]. As a result, the quantum efficiency ultimately decreases. Another reason may be due to agglomeration of the catalyst particles which then leads to reduced total surface area exposed to the incoming light. For further evaluation, the irradiation time is kept constant at 90 min since further increase of irradiation time slightly improves degradation efficiency.

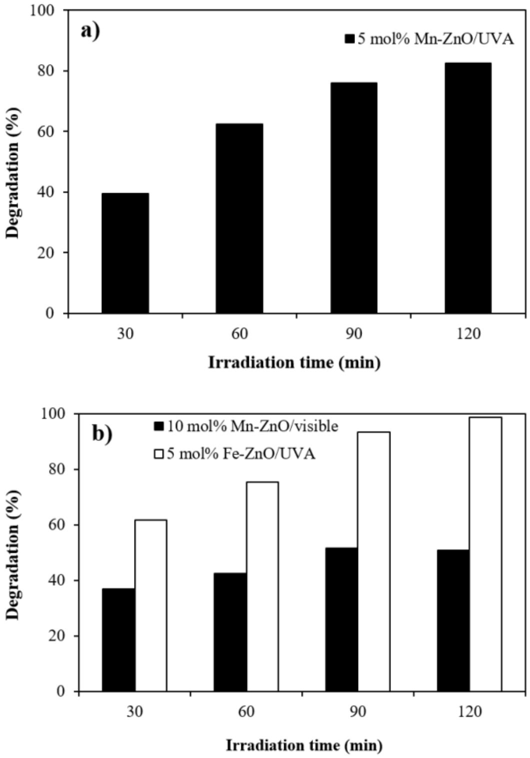

Figure 6. Effect of irradiation time on the degradation of MB (a) and AM (b) (pH = 7, catalyst concentration = 1 g/L, dye concentration = 10 mg/L).

3.3.3 Effect of pH

For evaluation of the effect of pH on the dye degradation, the initial pH of the suspension was varied (3, 5, 7, 9, and 11). The initial dye concentration was kept constant at 10 mg/L. As shown in Figure 7, the degradation efficiency of MB slightly increases from 80 to 86% when increasing pH from 3 to 5. The degradation efficiency then gradually decreases with further increases of pH from 5 to 11. Based on the literature, the surface of ZnO is positively charged at a pH below 7 and becomes negatively charged at a pH above 7 [28]. MB is a cationic dye whose high pH favours its adsorption on the ZnO surface, resulting in a high degradation under neutral and alkaline conditions. However, in this case, the stability of ZnO might not be guaranteed at high pH due to the possibility of alkaline dissolution [29]. Thus, it leads to low dye degradation at alkaline pH.

For the degradation of AM, when increasing pH from 3 to 7, the degradation efficiency generally increases. This is probably associated with susceptibility of the azo group to electrophilic attack by hydroxyl radicals. In low pH, the concentration of H^+ ions is in excess. H^+ ions can decrease the electron densities at the azo group. This means that the reactivity of hydroxyl radicals towards the azo group decreases. With further increases of pH from 7 to 11, the degradation efficiency generally decreases as well. AM is an anionic dye and the ZnO is negatively charged at high pH. Therefore, these cause repulsion between AM and the catalyst surface, resulting in ineffective AM adsorption and hence poor AM degradation.

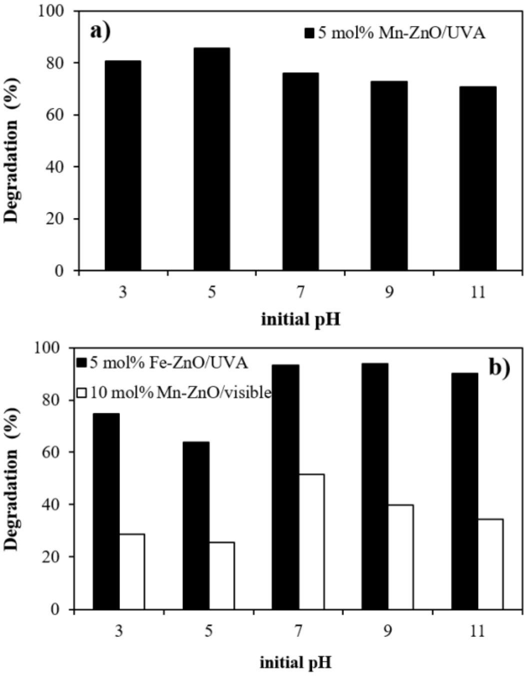

Figure 7. Effect of initial pH on the degradation of MB (a) and AM (b) (irradiation time = 90 min, catalyst concentration = 1 g/L, dye concentration = 10 mg/L).

3.4 Reusability

The reusability studies on the pristine (acet-ZnO), 5 mol% Mn-ZnO and 5 mol% Fe-ZnO for the degradation MB and AM at selected experimental conditions under UVA light were carried out. It is to be noted that the reusability of nit-ZnO is not performed since it possesses low photocatalytic activity. As shown in Figure 8, acet-ZnO shows better performances for the degradation of both AM and MB. It gives 98% of MB degradation in the first run. However, the MB degradation gradually decreases to 84% at the third run. In the other cases, the reusability is even worse. The low reusability can be because the catalyst particles are not easily separated from the solution and thus lost during recycle. In addition, there may be permanent adsorption of the dye degradation products on the catalyst surface which hinders the adsorption of dye and the absorption of light in subsequent degradation runs.

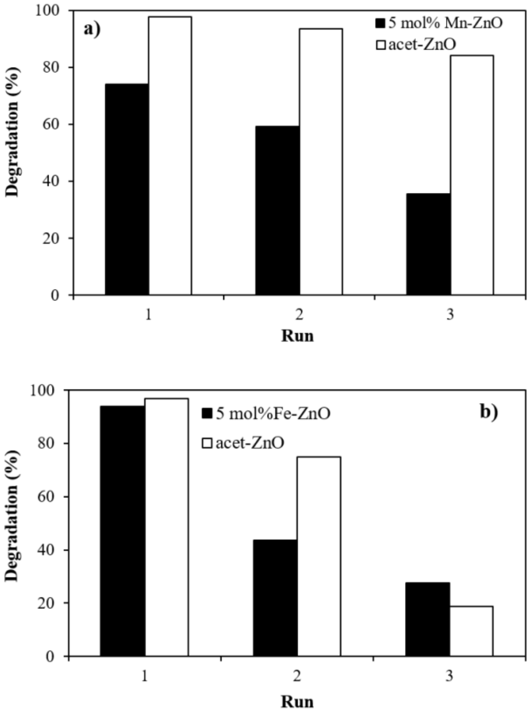

Figure 8. Reusability of pristine and doped-ZnO for degradation MB (a) and AM (b) under UVA light (catalyst concentration = 1 g/L, dye concentration = 10 mg/L, pH = 7, and irradiation time 90 min).

4. Conclusion

In summary, a series of Mn- and Fe-ZnO with various dopant contents are successfully synthesized using the modified sol-gel method. In general, Fe-ZnO is a better catalyst for the AM degradation under UVA and visible light, while Mn-ZnO is more effective for the MB degradation. The results also reveal that the dopant addition generally enhances the photocatalytic activity. The optimum doping content is mostly obtained at 5 mol%. Pristine ZnO prepared with zinc nitrate shows lower performances as compared to that prepared with zinc acetate. This is likely because of the contamination of sodium ion which blocks the pores and passivates the surface. Moreover, there is a difference in the dye degradation mechanism under visible light between Fe-ZnO and Mn-ZnO, which is most likely due to the difference in their surface properties. Overall, the developed catalysts, especially Fe-ZnO, are found to be promising for the degradation of recalcitrant dyes. Almost complete degradation of dyes can be achieved in a short period of treatment under UVA light. Therefore, both Fe-ZnO and Mn-ZnO can be used in a real setting for photocatalysis under solar light.

5. Acknowledgements

The authors would like to acknowledge the research funding and facilities provided by the Sirindhorn International Institute of Technology, Thammasat University.

6. References

[1] Garcia, J., Oliveira, J., Silva, A., Oliveira, C., Nozaki, J., and De Souza, N., Comparative Study of the Degradation of Real Textile Effluents by Photocatalytic Reactions Involving $UV/TiO_2/H_2O_2$ and $UV/Fe^{2+}/H_2O_2$

Systems, J. Hazard. Mater., Vol. 147, pp. 105-110, 2007.

[2] Lee, J-W., Choi, S-P., Thiruvenkatachari, R., Shim, W-G., and Moon, H., Evaluation of the Performance of Adsorption and Coagulation Processes for the Maximum Removal of Reactive Dyes. Dyes Pigm., Vol. 69, pp. 196-203, 2006.

[3] Behnajady, M.A., Modirshahla, N., Mirzamohammady, M., Vahid, B., and Behnajady, B., Increasing Photoactivity of Titanium Dioxide Immobilized on Glass Plate with Optimization of Heat Attachment Method Parameters. J. Hazard. Mater., Vol. 160, pp. 508-513, 2008.

[4] Sudrajat, H., and Babel, S., Comparison and Mechanism of Photocatalytic Activities of N-ZnO and N-ZrO_2 for the Degradation of Rhodamine 6G. Environ. Sci. Pollut. Res., Vol. 23, pp. 10177-10188, 2016.

[5] Bandala, E.R., Peláez, M.A., García-López, A.J., Salgado, M.D.J, Moeller, G. Photocatalytic Decolourisation of Synthetic and Real Textile Wastewater Containing Benzidine-Based Azo Dyes. Chem. Eng. Process, Vol. 47, pp. 169-176, 2008.

[6] Alinsafi, A., Evenou, F., Abdulkarim, E., Pons, M.-N., Zahraa, O., Benhammou, A., et al. Treatment of Textile Industry Wastewater by Supported Photocatalysis. Dyes Pigm., Vol. 74, pp. 439-445, 2007.

[7] Sudrajat H, Babel S. A New, Cost-Effective Solar Photoactive System N-ZnO@ Polyester Fabric for Degradation of Recalcitrant Compound in a Continuous Flow Reactor. Mater. Res. Bull., Vol. 83, pp. 369-378, 2016.

[8] Sudrajat, H., Babel, S., Sakai, H., and Takizawa, S., Rapid Enhanced Photocatalytic Degradation of Dyes using novel N-doped ZrO_2. J. Environ. Manage., Vol.165, pp. 224-234, 2016.

[9] Carraway, E.R., Hoffman, A.J., and Hoffmann, M.R., Photocatalytic Oxidation of Organic Acids on Quantum-sized Semiconductor Colloids. Environ. Sci. Technol., Vol. 28, pp. 786-793, 1994.

[10] Pal, B., and Sharon, M., Enhanced Photocatalytic Activity of Highly Porous ZnO Thin Films Prepared by Sol–gel Process, Mater. Chem. Phys., Vol. 76, pp. 82-87, 2002.

[11] Jung, K.Y., Kang, Y.C., and Park, S.B., Photodegradation of Trichloroethylene Using Nanometre-Sized ZnO Particles Prepared by Spray Pyrolysis. J. Mater. Sci. Lett., Vol. 16, pp. 1848-1849, 1997.

[12] Sakthivel, S., Neppolian, B., Shankar, M., Arabindoo, B., Palanichamy, M., and Murugesan, V., Solar Photocatalytic Degradation of Azo Dye: Comparison of Photocatalytic Efficiency of ZnO and TiO_2. Sol. Energ. Mat. Sol. Cells., Vol. 77, pp. 65-82, 2003.

[13] Ullah, R., and Dutta, J., Photocatalytic Degradation of Organic Dyes with Manganese-doped ZnO Nanoparticles. J. Hazard. Mater., Vol. 156, pp. 194-200, 2008.

[14] Saleh, R., and Djaja, N.F., UV Light Photocatalytic Degradation of Organic Dyes with Fe-doped ZnO Nanoparticles, Superlattices and Microstruct., Vol. 74, pp. 217-233, 2014.

[15] Lin, S-S., Huang, J-L., and Lii, D-F., Effect of Substrate Temperature on the Properties of Ti-doped ZnO Films by Simultaneous rf and dc Magnetron Sputtering. Mater. Chem. Phys., Vol. 90, pp. 22-30, 2005.

[16] Park, J.Y., Lee, D.J., Yun, Y.S., Moon, J.H., Lee, B-T., and Kim, S.S., Temperature-induced Morphological Changes of ZnO Grown by

Metalorganic Chemical Vapor Deposition. J. Cryst. Growth, Vol. 276, pp. 158-164, 2005.

[17] Demyanets, L., Li, L., and Uvarova, T., Hydrothermal Synthesis and Cathodoluminescence of ZnO Crystalline Powders and Coatings. J. Cryst. Growth, Vol. 287, pp. 23-27, 2006.

[18] Gupta, V., Suhas, Ali, I., Saini, V. Removal of Rhodamine B, Fast Green, and Methylene Blue from Wastewater Using Red Mud, an Aluminum Industry Waste. Ind. Eng. Chem. Res., Vol. 43, pp. 1740-1747, 2004.

[19] Mak, S.-Y., Chen, D.-H. Fast Adsorption of Methylene Blue on Polyacrylic Acid-bound Iron Oxide Magnetic Nanoparticles. Dyes Pigm., Vol. 61, pp. 93-98, 2004.

[20] Jimenez-Gonzalez, A., Urueta, J.A.S., and Suarez-Parra, R., Optical and Electrical Characteristics of Aluminum-doped ZnO Thin Films Prepared by Solgel Technique. J. Cryst. Growth, Vol. 192, pp. 430-438, 1998.

[21] Zhang, X., Qin, J., Hao, R., Wang, L., Shen, X., and Yu, R., Carbon-Doped ZnO Nanostructures: Facile Synthesis and Visible Light Photocatalytic Applications, J. Phys. Chem. C, Vol. 119, pp. 20544-20554, 2015.

[22] Li, Y., Peng, S., Jiang, F., Lu, G., and Li, S., Effect of Doping TiO_2 with Alkaline-earth Metal Ions on Its Photocatalytic Activity. J. Serb. Chem. Soc., Vol. 72, 393-402, 2007.

[23] Barick, K., Singh, S., Aslam, M., and Bahadur, D., Porosity and Photocatalytic Studies of Transition Metal Doped ZnO Nanoclusters. Micropor. Mesopor. Mater., Vol. 134, pp. 195-202, 2010.

[24] Lupan, O., Pauporté, T., Le Bahers, T., Viana, B., and Ciofini, I., Wavelength-Emission Tuning of ZnO Nanowire-Based Light-emitting Diodes by Cu doping: Experimental and Computational Insights. Adv. Funct. Mater., Vol. 21, pp. 3564-3572, 2011.

[25] Liu, G., Zhang, X., Xu, Y., Niu, X., Zheng, L., and Ding, X.. The Preparation of Zn^{2+}-doped TiO_2 Nanoparticles by sol–gel and Solid Phase Reaction Methods Respectively and Their Photocatalytic Activities. Chemosphere, Vol. 59, pp. 1367-1371, 2005.

[26] Akpan, U., and Hameed, B., Parameters Affecting the Photocatalytic Degradation of Dyes Using TiO_2-based Photocatalysts: a Review. J. Hazard. Mater., Vol. 170, pp. 520-529, 2009.

[27] Choi, W., Termin, A., and Hoffmann, M.R., The Role of Metal Ion Dopants in Quantum-sized TiO_2: Correlation between Photoreactivity and Charge Carrier Recombination Dynamics. J. Phys. Chem., Vol. 98, pp. 13669-13679, 1994.

[28] Akyol, A., Yatmaz, H., and Bayramoglu, M., Photocatalytic Decolorization of Remazol Red RR in Aqueous ZnO Suspensions. Appl. Catal. B, Vol. 54, pp. 19-24, 2004.

[29] Han, J., Qiu, W., and Gao, W., Potential Dissolution and Photo-dissolution of ZnO Thin Films. J. Hazard. Mater., Vol. 178, pp. 115-122, 2010.